Experimental Characterization of Passively Damped Joints for Space Structures

Jacky Prucz*
West Virginia University, Morgantown, West Virginia
A. D. Reddy† and L. W. Rehfield‡
Georgia Institute of Technology, Atlanta, Georgia
and
R. W. Trudell§
McDonnell Douglas Astronautics Company, Huntington Beach, California

An innovative means to enhance the inherent damping in structures is provided by the designed-in incorporation of viscoelastic materials in joints. The damping and stiffness properties of such joints have been experimentally evaluated at room temperature and low frequencies on representative specimens. The test data show that proper design configurations can yield significant damping benefits without unacceptable stiffness penalties. Three different test methods and a new data reduction procedure have been utilized in the experimental program. Two of the three methods are new. A simplified steady-state technique and a sine-pulse propagation approach have been developed and applied in this research. The results show relatively low data scatter from repeated measurement sets, and there is good agreement among the different test methods.

Nomenclature

A = amplitude of displacement output from exciter
A_v = shear area of viscoelastic layer
B = amplitude of load signal
C = equivalent compliance of test set-up
C_m = wave velocity in reference homogeneous specimen
C_j = wave velocity in joint specimen
$D_j(t)$ = time signal of joint damping effect
E_m = extensional modulus of member
G_1 = storage shear modulus of viscoelastic material
G_2 = dissipative shear modulus of viscoelastic material
G_M = magnitude of complex shear modulus
H_a = hysteresis loop area
L_m = member length in test specimen
L_j = joint length in test specimen
K_m = axial stiffness of member
K_j = axial stiffness of joint
K = axial stiffness of reference homogeneous specimen
K_v = equivalent stiffness of viscoelastic layer
K_1 = internal stiffness of exciter
K_2 = load cell stiffness
K_3 = test fixture stiffness
M_f = merit factor
$P_1(t)$ = input load signal for reference specimen
$P_{1j}(t)$ = input load signal for joint specimen
$P_2(t)$ = output load signal for reference specimen
$P_{2j}(t)$ = output load signal for joint specimen
$P_{\max}$ = external load amplitude
$R_j(t)$ = time signal of direct joint reflections
U_1, U_2 = total input and output energy of sine pulse, respectively
$U_{\max}$ = maximum strain energy stored per cycle
t_i = digital time variable
t_v = thickness of adhesive layer
Δt = propagation time of pulse front
α = reflection parameter
η_e = damping efficiency parameter
η = loss factor of reference homogeneous specimen
η_j = loss factor of joint specimen
θ = phase angle between voltage and load signals

Presented as Paper 85-780 at the AIAA/ASME/ASCE/AHS Structures, Structural Dynamics and Materials Conference, Orlando, FL, April 15-17, 1985; received Aug. 12, 1985; revision received Jan. 31, 1986.

*Assistant Professor, Mechanical and Aerospace Engineering.
†Senior Research Engineer, School of Aerospace Engineering.
‡Professor, School of Aerospace Engineering.
§Principal Engineer Scientist.

Introduction

THE current interest in large space structures has spawned applied research and development efforts in the vibration control area. Active modal control approaches have been considered the primary means to obtain sufficient energy dissipation and motion management in these structures. However, their application uncertainties, especially in the area of wide-band control effectiveness and cost, have directed recently increasing attention to the old subject of passive structural damping.[1] Consequently, passive damping enhancement is considered today a key element of any successful vibration control approach.

High passive damping not only limits vibration amplitudes and shortens transient decay times, but also has favorable synergistic effects when combined with active controls. The performance of active modal control systems is enhanced significantly due to improved control system error tolerance, reduced levels of disturbances, and reduced control bandwidth requirements.[2]

The use of viscoelastic materials for the control of structural vibrations has been an approach used in an ever increasing variety of applications, as viscoelastic technology becomes well established and more widely known. The literature is replete with examples of constrained-layer viscoelastic damping treatments applied over large areas and viscous dampers applied to problem components.[3,4] While generally successful, some penalties are usually attendant because of the add-on approach typical of past applications. Damping treatments have been used as cures for unforseen problems and therefore have been afterthoughts.

An innovative means to enhance the inherent damping in structures is provided by the designed-in incorporation of viscoelastic materials in joints. It combines the well-known damping capability of viscoelastic materials with the predominant influence that joints and supports have on the overall

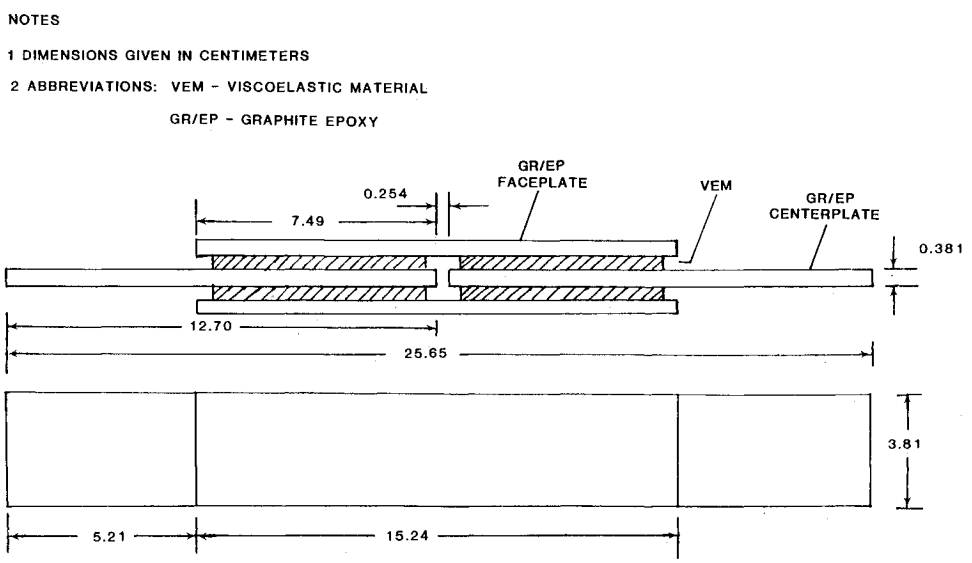

Fig. 1 Passively damped joint specimen without elastic link between members.

damping of most structures.[5] The designed-in approach provides a promising opportunity to maximize the damping benefit while minimizing the associated penalties in other structural properties. Preliminary theoretical and experimental research has been undertaken in the last two years for the development of passively damped joining concepts for space structures. New analytical models and experimental methods have been developed for the mechanical performance analysis of such joints and have been reported in Refs. 6-8. This paper covers only selected experimental results, its major objective being the presentation of typical damping and stiffness data from basic space structure damped joint concepts and the various methods used to obtain them.

Certain particular features of passively damped joints, like large vs small motion effects, nonhomogeneity, significant frequency and temperature dependence of their mechanical properties, impose an unusual variety of requirements on their experimental evaluation. Generic and accurate test results are required when the properties of the overall structure are synthesized from those of its components. They need to be acquired over a wide and continuous range of expected frequencies and ambient temperatures in order to account for the possible changes caused by these factors in the viscoelastic material properties.[9]

Many experimental techniques have been developed in the past for the dynamic characterization of structural materials and components.[10-12] However, none of the conventional approaches seems to fulfill all the test data requirements imposed by the various modeling approaches for passively damped joints.[6] Two new testing methods consequently have been developed for this research program, although their simplicity and reliability make them attractive for extended applications in the areas of material qualifications and structural characterizations. They are a simplifed, non-resonant forced vibration approach and a stress-pulse propagation approach, which have been previously presented in Refs. 6, 7, and 13 and are briefly described in this paper.

Since the primary candidates for large space structures are repetitive lattice trusses, the main loading direction considered in the design and testing of passively damped joint specimens is the axial one. The tests are limited to the 0.1-100 Hz frequency range and low strain levels, which are expected to be dominant in these structures.[2] Although environmental testing over a temperature range of $-150°F$ to $400°F$ is also included in the program, only room temperature data are presented in this paper.

Test Specimens

Fifteen specimens of passively damped joints have been fabricated for experimental evaluation. They are based on a symmetric double lap configuration in which the damping enhancement is achieved by shear deformation of the viscoelastic adhesive layers when the joint members are loaded in their axial direction (Fig. 1). Three specimens include a direct glass-fiber connection between the members for improved minimum stiffness and structural redundancy at elevated temperatures, or in the case of viscoelastic materials with poor creep resistance (Fig. 2).

Six different types of viscoelastic materials, which are being considered for space applications, have been used in the specimens. Their trade names, chemical base, and manufacturer are given in Table 1. In all the specimens with glass-fiber elements, the epoxy-based EC 2216 material is used for the adhesive layers. The other 12 specimens are grouped in pairs,

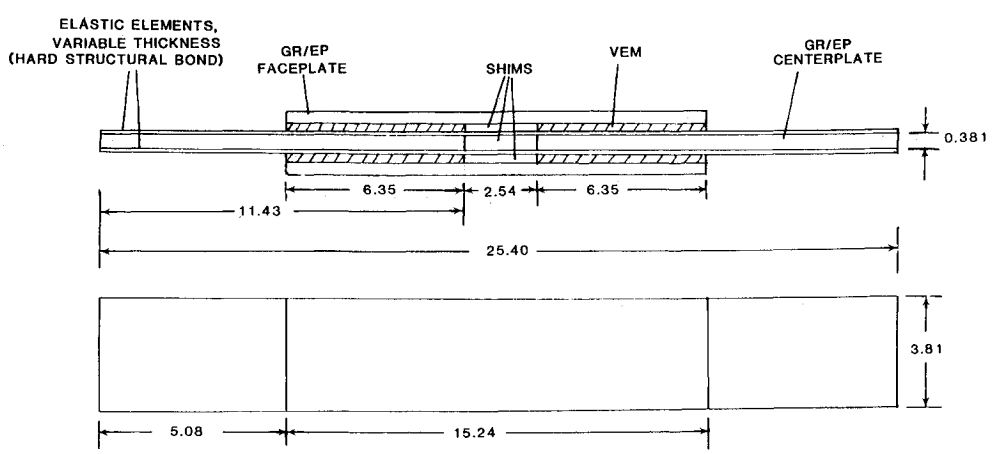

Fig. 2 Passively damped joint specimen with elastic elements.

since two identical specimens have been built for each type of viscoelastic material. Only the relevant mechanical properties of these materials are discussed here, although their chemical stability and processing procedures were considered in their selection for space applications. Room temperature hysteresis testing of all 15 specimens revealed no significant differences between the two specimens grouped in the same pair. Therefore, only the seven specimens listed in Table 1 have been selected for extensive experimental investigation and for discussion in this paper. In order to provide a practical reference base for the performance evaluation of passively damped joints, a standard double lap bonded joint with highly rigid epoxy adhesive layers has been included in the testing program and in Table 1.

The design of the test specimens has been guided by two major criteria[7]: 1) The ultimate strength of the joint should be at least 1/10 that of a longeron in a space truss. 2) When elastic elements are included in the joint, as shown in Fig. 2, the equivalent shear stiffness of the adhesive layers should be equal to the axial stiffness of the elastic elements in order to provide the maximum damping for the minimum stiffness loss. Assuming that the shear stress in each adhesive layer is uniformly distributed over its surface, the equivalent shear stiffness can be approximately calculated as follows:

$$K_v = (G_M A_v)/(t_v) \tag{1}$$

where

$$G_M = (G_1^2 + G_2^2)^{1/2} \tag{2}$$

This simple model is sufficient for design when $G_M \ll E_m$. It works well for design sizing of the joints listed in Table 1. Detailed joint models for the case where G_M approaches E_m are given in Refs. 7, 8, and 13.

Experimental Apparatus and Procedures

The damping and stiffness characteristics of selected test specimens have been measured by three different methods. This multiple method approach not only enhances the statistical confidence in the results, but also provides a reliable data base for correlation between the various testing techniques. In addition to the new steady-state and transient methods, the classical hysteresis-loop technique has been included in the experimental program. New and innovative data acquisition and reduction procedures, based on advanced digital instrumentation, have been utilized for all three selected techniques.

Hysteresis-Loop Approach

The experimental set-up used for the hysteresis-loop technique is shown in Fig. 3. The specimen is mounted vertically in an Instron Universal Testing Machine and a cyclic axial load is applied to it by the moving, lower crosshead of the machine. A strain gage load cell built in the fixed upper crosshead measures the resultant load on the specimen. The relative axial displacement between the edges of the joint section of the specimen is measured by a LVDT (linear variable differential transformer) extensometer. Three different loading rates have been tested for each specimen by presetting the vertical speed of the lower crosshead to 0.127, 0.254, and 0.508 cm/s (0.05, 0.1, and 0.2 in./s, respectively). However, the resultant loading frequencies cannot be directly controlled and they are higher for stiffer specimens, even at the same speed of the crosshead.

The load and displacement time histories are acquired and stored as voltage signals on separate channels of a Nicolet 4094A digital oscilloscope, after preliminary electronic filtering and amplification. The digital data reduction is performed on an HP 9845B desk computer after the automatic transfer of the measured voltage signals from the memory unit of the Nicolet oscilloscope through a General Purpose Interface Bus system (GPIB).

The ratio between the maximum axial load and the maximum axial deformation yields the corresponding stiffness of the specimen. The damping characteristic is expressed in terms of the loss factor, which can be determined either from the phase shift between the zero crossings of the load and displacement variations with time, or from the area enclosed inside the resultant hysteresis-loop. The second alternative has been chosen here since it does not require a high time resolution of the processed signals. The corresponding expression of the loss factor is[9]:

$$\eta_j = (H_a)/(2\pi U_{\max}) \tag{3}$$

where the hysteresis loop area H_a is evaluated by numerical integration of the measured data in the load-displacement plane. The maximum stain energy stored in one cycle, $U_{\max}$, is given by

$$U_{\max} = (P_{\max}^2)/(2K_j) \tag{4}$$

Simplified Steady-State Approach

The experimental set-up utilized for the simplified steady-state method is shown in Fig. 4. A special piezoelectric displacement transducer has been developed for this purpose. Its major requirement is to provide a displacement output proportional to the voltage input for dynamic excitation of specimens from 0.1 to 100 Hz. Therefore, complex modulus data can be generated without independent measurements of relative displacements, as in conventional non-resonant forced vibration techniques. This is why the new method is considered "simplified," an especially attractive feature for space

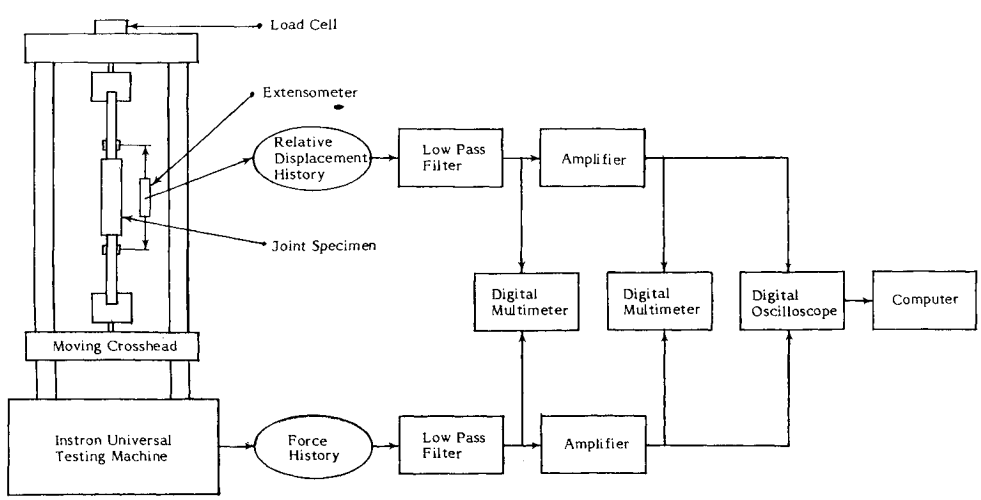

Fig. 3 Experimental set-up for the hysteresis-loop approach.

structures where elastic displacements normally are expected to be small.

A harmonic voltage applied to the piezoelectric exciter generates a small axial harmonic motion, which is transmitted through the test specimen, resulting in an axial harmonic force measured by the piezoelectric load cell. The complex stiffness of the specimen is determined from the following expressions:

$$\mathrm{Re}(K_j) = \frac{1}{\Delta}\left(\frac{B}{A}\cos(\theta) - \frac{B^2}{A^2}C\right) \tag{5}$$

$$\mathrm{Im}(K_j) = \frac{1}{\Delta}\frac{B}{A}\sin(\theta) \tag{6}$$

where

$$\Delta = 1 - 2C\frac{B}{A}\cos(\theta) + C^2\left(\frac{B}{A}\right)^2 \tag{7}$$

$$C = \sum_{i=1}^{3}\frac{1}{K_i} \tag{8}$$

Equations (5) and (6) directly yield the loss factor:

$$\eta_j = [\mathrm{Im}(K_j)]/[\mathrm{Re}(K_j)] \tag{9}$$

The displacement amplitude, A, corresponds to the output motion of the exciter in the unloaded condition, i.e., with no specimen attached to it. In the loaded condition, the corresponding amplitude departs from A because the internal stiffness of the transducer is not infinite. The actual motions are determined from the equilibrium condition between the external reaction force and the internal force generated by the piezoelectric effect. The equivalent compliance C in the above equations is a correction term that accounts for the stiffness contributions of the test fixture, load cell, and displacement transducer. It can be neglected when the stiffness of the specimen is much lower than the combined stiffness of these elements.

Preliminary dynamic tests have been conducted for the sensitivity and internal stiffness evaluation of the piezoelectric motion transducer. The simplified steady-state method has been applied to the joint specimens by using these data in Eqs. (5-8). The time histories of the voltage applied to the exciter and the load cell response are acquired, averaged, and analyzed on separate channels of the Nicolet 4094A digital oscilloscope. After elimination of the DC components from the two signals, the displacement amplitude A and the force amplitude B are calculated by using the appropriate calibration factors. The load phase lag, θ, with respect to the applied displacement, is determined by the difference between the zero-crossings of the corresponding time waves. The direct data analysis on the digital oscilloscope is preferred here over transmission and analysis on the computer because of the high time resolution required for accurate phase shift measurements.

Sine-Pulse Propagation Approach

No custom-built test fixture or exciter is needed for application of the sine-pulse propagation method. Nevertheless, the facilities developed for the simplified steady-state technique have been used also for the transient tests in order to facilitate data correlation between the two methods. The corresponding experimental set-up is shown in Fig. 5. The voltage signal applied to the piezoelectric exciter is supplied and amplified by the same equipment as in the simplified steady-state tests, but the continuous sine wave generated by the function generator is now gated to the desired pulse length. All the excitation pulses used in the tests contain just one full cycle. The stiffness and damping properties of the test specimen are determined by comparing the response signals from two identical PCB piezoelectric load cells mounted at its ends.

After passing through two identical AVL charge amplifiers, these signals are acquired on separate channels of a Nicolet 4094A digital oscilloscope. The data reduction is performed, like in the hysteresis-loop technique, on an HP 3845B desk computer. The input and output load signals acquired for each test are transferred separately through the GPIB interface system from the memory unit of the Nicolet oscilloscope to the computer memory. The damping performance can be expressed in terms of a general "damping efficiency" parameter, which is defined as follows:

$$\eta_e = (U_1 - U_2)/(U_1) \tag{10}$$

Since each data point in the measured digital signals represents an axial load, the total strain energy levels associated with the input and output pulses may be expressed, respectively, as

$$U_1 = \frac{1}{2K_j}\sum_{t_i=1}^{T}\left[\frac{2\alpha}{\alpha+1}P_{1j}(t_i)\right]^2 \tag{11}$$

$$U_2 = \frac{1}{2K_j}\sum_{t_i=1}^{T}\left[\frac{2\alpha}{\alpha+1}P_{1j}(t_i) + D_j(t_i)\right]^2 \tag{12}$$

where the summation symbols denote numerical time integrations over the pulse length T.

The parameter α in these equations accounts for the fact that in the case of a joint specimen, the measured load signals include the effects of wave reflections and refractions at the joint-member discontinuity interfaces.[14] Force equilibrium and displacement continuity conditions at these interfaces dictate the signs and amplitudes of the resulting waves as a function of a reflection parameter, which may be defined as

$$\alpha = \frac{C_m}{C_j}\frac{L_j}{L_m}\frac{K_j}{K_m} \tag{13}$$

where the index m refers to the member and the index j refers to the joint portion of the test specimen.

Since the joint damping affects only that part of the applied load that is transmitted through the joint, the reflection parameter α must be evaluated before the damping effect can be separated from the measured signals. For this purpose, the input load signal of the joint specimen is compared with a reference input load signal for the same applied excitation. The reference specimen is an homogeneous bar with the same geometrical and material characteristics as the members of the joint specimen, so that the difference between the two signals is mainly due to the reflection at the member-joint interface, i.e.

$$-R_j(t_i) = |P_1(t_i) - P_{1j}(t_i)| \tag{14}$$

The parameter α is approximately evaluated from the equation[13,14]

$$\alpha = \frac{1 - \mathrm{AVE}[R_j(tr_i)/P_1(t_i)]}{1 + \mathrm{AVE}[R_j(t_i)/P_1(t_i)]} \tag{15}$$

where AVE denotes a numerical time averaging operator over the pulse length. The damping effect of the joint is subsequently determined as follows:

$$D_j(t_i) = \mathrm{FIT}[P_{2j}(t_i) - P_{1j}(t_i)] - \left[1 - \frac{4\alpha}{(\alpha+1)^2}\right]P_{1j}(t_i) \tag{16}$$

FIT denotes a least-square fitting routine for the elimination of the effect of multiple reflections at the ends of the specimen.[7,13] Equation (16) is derived by considering the ma-

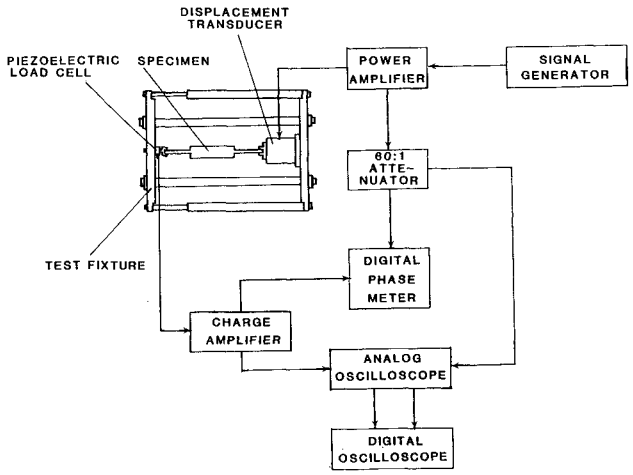

Fig. 4 Experimental set-up for the simplified steady-state approach.

jor reflection effects superposed in the measured load signals $P_{1j}(t)$ and $P_{2j}(t)$ and by extracting the damping signal $D_j(t)$ from their difference.

The axial stiffness of the reference homogeneous specimen K is evaluated from the propagation velocity of the applied stress pulse through this specimen C_m. The time delay Δt between the moments in which the pulse front reaches the two load cells is measured with an accuracy of about 1 μs when the data are acquired by the Nicolet 4094A oscilloscope at its maximum sampling rate. In the case of a joint specimen, the axial stiffness K_j is evaluated approximately by using Eq. (13), where the wave velocity C_j is determined separately, like C_m, by measuring the propagation time of the pulse front between the two load cells.

Results and Discussion

Damping and Stiffness Characteristics

The hysteresis test data provide a representative picture about the damping and stiffness properties of the passively

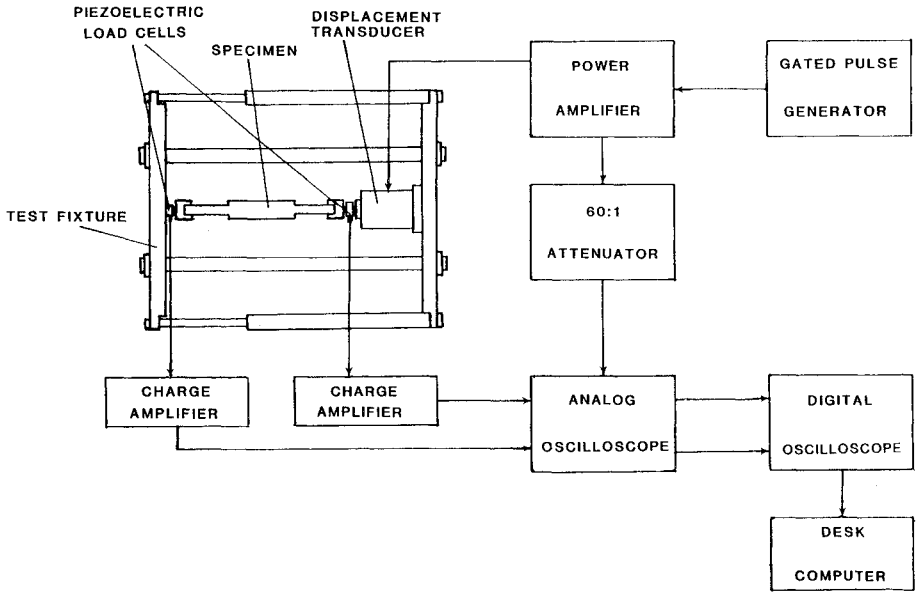

Fig. 5 Experimental set-up for the sine-pulse propagation approach.

Table 1 Viscoelastic materials and weight properties of test specimens

Specimen number	Viscoelastic material: Manufacturer	Name	Chemical base	Density, gm/cc (lb/in.^{3})	Thickness of adhesive layer, cm(in.)	Total mass,[a] kg(lb)
14[b]		EA956	Epoxy		0.0559 (0.0220)	0.130 (0.287)
1	3M	ISD 110	Acrylic	0.964 (0.0347)	0.0157 (0.0062)	0.124 (0.273)
3	3M	EC 2216	Epoxy	1.289 (0.0464)	0.3200 (0.1260)	0.167 (0.368)
5	Soundcoat	DYAD 606	Polyurethane	0.964 (0.0347)	0.1308 (0.0515)	0.109 (0.241)
7	Hysol	EA 9326	Polyurethane	1.080 (0.0389)	0.1219 (0.0480)	0.136 (0.299)
9	G.E.	SMRD 100F90	Epoxy	0.800 (0.0288)	0.1473 (0.0580)	0.126 (0.277)
11	G.E.	RTV 630	Silicone	1.280 (0.0461)	0.0185 (0.0073)	0.125 (0.275)
15[c]	3M	EC 2216	Epoxy	1.289 (0.0464)	0.1455 (0.0573)	0.153 (0.337)

[a]The density of the graphite/Epoxy faceplates is 1.511 gm/cc (0.0544 lb/in.^{3}). [b]Standard bonded joint with elastic adhesive. [c]Includes two 0.0597-cm (0.0235-in.) thick fiberglass strips with a density of 1.719 gm/cc (0.0619 lb/in.^{3})

damped joint specimens listed in Table 1, at very low frequencies. They enable both a comparative evaluation between the different design configurations and an illustration of typical performance characteristics of passively damped joints as compared with a reference homogeneous specimen (specimen 13, Table 2). The results presented in Table 2 correspond to the lowest motion speed of the Instron's crosshead, i.e., 0.127 cm/s (0.05 in./s). The resultant loading frequencies generally are higher for stiffer specimens, since the slope of their load vs displacement curve is higher. The interpretation of these results for practical applications is facilitated by considering their relative values with respect to the reference specimen, as shown in Table 3. The "damping benefit" is the ratio between the loss factor of the joint and that of the reference specimen, whereas the "stiffness penalty" is calculated as the ratio between the stiffness of the reference specimen and that of the joint. A combined parameter, which is labeled "merit factor" in Table 3, can be defined as

$$M_f = (\eta_j K_j)/(\eta K) \tag{17}$$

Because the specimens are all the same size, it can be interpreted as the damping benefit that is achievable with a given design configuration per unit value of stiffness penalty. The stiffness could also be improved by reducing the adhesive layer thickness when feasible.

The only two specimens with a merit factor higher than 1 are specimens 3 and 15, which both include the EC 2216 viscoelastic material as adhesive layers. The elastic glass-fiber elements included in specimen 15 reduce the stiffness penalty to less than half the stiffness penalty of specimen 3, but at the cost of an even higher reduction in the damping benefit. The ISD 110 viscoelastic material used in specimen 1 provides the highest damping enhancement, but its merit factor is low because of the serious reduction in stiffness. A thinner bond line is probably not practical in this case. The other materials do not display good damping-stiffness tradeoffs at these low frequencies either because of poor damping performance, like that of EA 9326 and RTV 630, or high stiffness penalty, like that associated with DYAD 606. However, the DYAD 606 could possibly be cast in thinner layers to reduce the stiffness loss.

The frequency effect on the damping and stiffness characteristics of selected specimens is shown in Figs. 6 and 7, respectively. These figures are based on test data generated by the simplified steady-state approach. A least-square fitting routine is used for drawing the "best fit" line between the data points of the same specimen. Three representative specimens of passively damped joints have been selected for Figs. 6 and 7, along with the standard elastic joint (specimen 14). Specimens 1 and 3 represent, respectively, the behavioral pattern associated with soft and stiff viscoelastic materials. The comparison between specimens 3 and 15 illustrates the effect of the elastic glass-fiber strips on the performance of a passively damped joint with stiff viscoelastic layers.

It should be emphasized that the damping data in Fig. 6 are expressed in terms of the measured loss factor of the joint rather than the material loss factor of the viscoelastic layers. The damping characteristics of soft joints, like specimen 1, are dominated by those of the adhesive materials, but as these materials become stiffer, the joint loss factor is reduced from the damping material loss factor since the viscoelastic layers share less of the total strain energy stored in the joint.[8,13] The

Table 2 Hysteresis-loop results at very low frequencies[a]

Specimen number	Frequency, Hz	Loss factor	Axial stiffness N/cm (lb/in.)
13[b]	0.078	0.035	825,520 (471,200)
1	0.033	0.567	12,280 (7,000)
3	0.070	0.454	311,280 (177,670)
5	0.016	0.281	30,050 (17,150)
7	0.072	0.033	335,560 (191,540)
9	0.044	0.099	120,370 (68,710)
11	0.033	0.029	73,850 (42,150)
15	0.077	0.163	761,690 (434,760)

[a]Motion speed of the Instron's crosshead preset at 0.127 cm/s (0.05 in./s).
[b]Reference homogeneous specimen with the same graphite/epoxy laminate as the faceplates of the joint specimens and the same cross section.

Table 3 Relative[a] performance parameters of passively damped joints

Specimen number	Damping benefit	Stiffness penalty	Merit factor
1	15.983	67.246	0.238
3	12.783	2.652	4.820
5	7.910	27.468	0.288
7	0.924	2.460	0.376
9	2.783	6.858	0.405
11	0.828	11.178	0.074
15	4.583	1.084	4.228

[a]With respect to the reference specimen data given in Table 2.

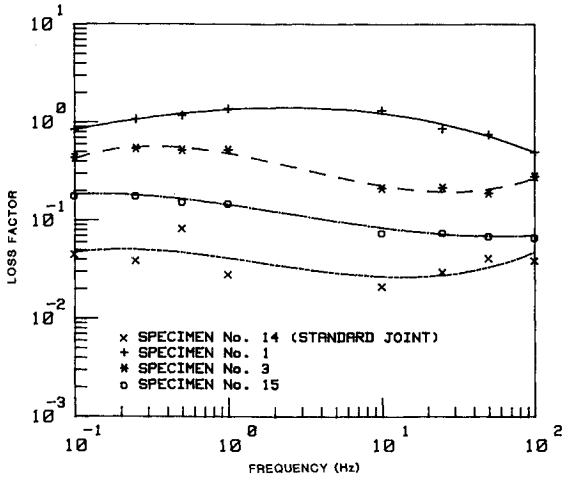

Fig. 6 Frequency effect on loss factor of joint specimens.

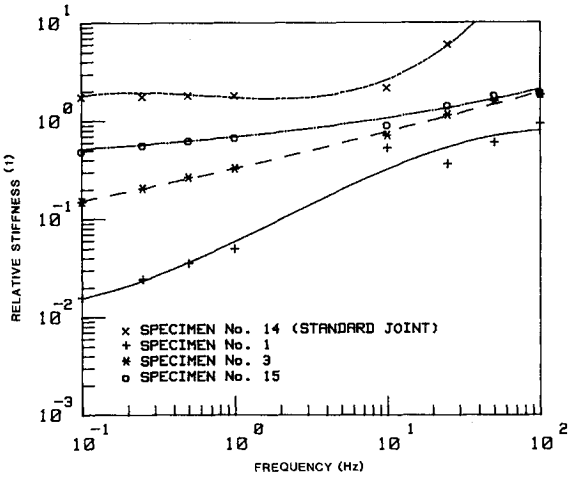

Fig. 7 Frequency effect on axial stiffness of joint specimens.

Table 4 Data correlation for hysteresis-loop tests

Specimen number	Final data[a] G_2/G_1	Final data[a] G_1 Pa × 10⁻³ (psi)	Preliminary data[b] G_2/G_1	Preliminary data[b] G_1 Pa × 10⁻³ (psi)	Other available data Source	Other available data G_2/G_1	Other available data G_1 Pa × 10⁻³ (psi)
1	0.622	90 (13.20)	0.725	60 (9.00)	UDRI[c]	0.65	120 (17.0)
3	0.454	33,210 (4820)	0.286	17,360 (2520)	ANATROL	0.15	21,030 (3050)
5	0.469	3140 (455)	0.498	4320 (630)	UDRI	0.53	990 (145)
7	0.033	15,680 (2270)	0.046	21,720 (3150)			
9	0.156	7510 (1090)	0.218	6970 (1010)	GE[d]	0.07	11,030 (1600)
11	0.077	540 (78)	0.074	570 (82)			

[a]Measured by Georgia Institute of Technology. [b]Measured by McDonnel Douglas Astronautics Company. [c]University of Dayton Research Institute. [d]General Electric.

stiffness increase with frequency, as illustrated in Fig. 7, may yield, therefore, a reduction in the damping performance of the joint at higher frequencies even for a viscoelastic material with a relatively flat loss factor-frequency behavior. One may also notice that the reduced stiffness penalties at frequencies above 10 Hz will improve significantly the merit factors given in Table 3, especially for the softer materials like the ISD 110 used in specimen 1.

Test Data Correlation

The hysteresis test results have been correlated with available data on the viscoelastic materials listed in Table 1 by using the approximate expression (1) in order to relate the measured joint characteristics to the corresponding material properties. The results of preliminary hysteresis tests performed on the same specimens[7] are also included in this correlation. The loss factors and storage shear moduli evaluated by the different sources for each material candidate are given in Table 4. It should be emphasized that this is only a gross comparison among the various data sources, primarily because the test frequencies do not coincide with each other. The frequencies of the preliminary tests have been selected as a common reference—only those data of the final tests that were measured at the closest frequencies to these references are included in Table 4, whereas the material data available from other sources have been extrapolated to the reference frequencies.[7] Satisfactory agreement is found, in general, between the different data sources in Table 4, considering the approximate way in which the material properties have been calculated from the joint specimen data, the different testing conditions, and the high scatter usually encountered in damping test results.[15]

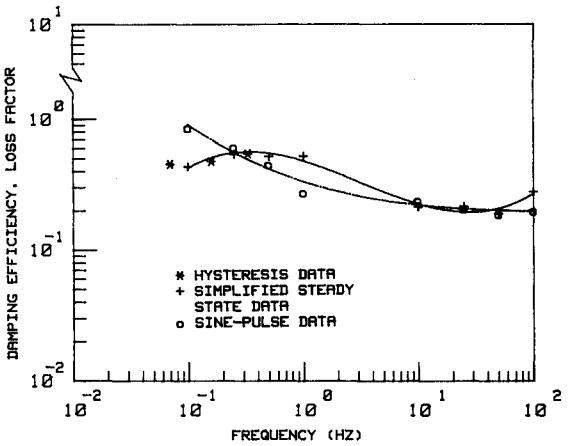

Fig. 8 Damping data correlation for specimen No. 3.

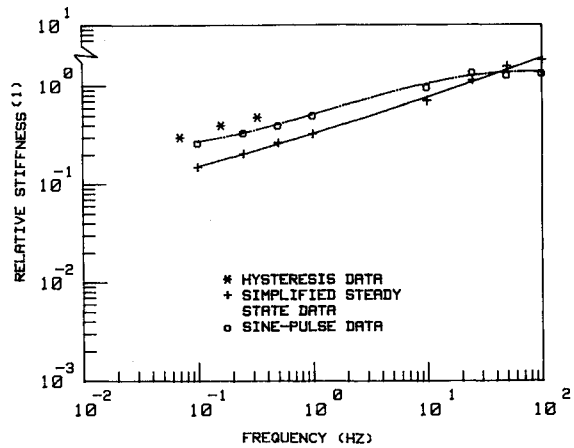

Fig. 9 Stiffness data correlation for specimen No. 3.

The data correlation between the three testing approaches previously described is illustrated in Figs. 8 and 9 for specimen 3. These figures show, in general, good agreement between the various methods and rational behavior within each method. Successive measurements on the same specimens, in the same testing conditions, showed an extremely high repeatability of the corresponding digital signals. Each experimental result presented in this paper is based on an average of at least 10 successive signals with a very low standard deviation. The lower stiffness values yielded by the simplified steady-state technique in the 0.1-1 Hz frequency range indicate that the unloaded sensitivity of the piezoelectric displacement transducer may be slightly lower than the average value extrapolated to this range from calibration test data measured at 10 Hz.[13] The "damping efficiency" parameter associated with the sine-pulse propagation approach provides a general measure of damping, which is not restricted to oscillatory loading like the commonly used "loss factor" parameter. Figure 8 shows that the numerical values and the general trends described by these parameters are relatively close, although they are generated by different testing and analysis techniques. The simplified steady-state method has been selected for the comparative evaluation of the test specimens in the previous section since it is more closely related to conventional measurement and interpretation concepts of damping data than the sine-pulse propagation technique.

Conclusions

Passively damped joints provide a cheap, simple, and efficient means to enhance the inherent damping in space structures. Favorable tradeoffs between the damping benefit and the associated stiffness penalty can be achieved if the

designed-in approach is adopted. This possibility is well reflected in the test data for specimen 15, although better tradeoffs can be achieved with improved design configurations.

The two new testing methods developed during this program, namely the simplified steady-state and the sine-pulse propagation, are useful and reliable tools for dynamic characterization of structural materials and components. The first is based on the conventional approach of non-resonant forced vibrations, but it has the advantage that no measurement of relative displacement is needed for the complex modulus evaluation. This permits measurements of joint properties at extremely small displacements. The sine-pulse method employs a wave propagation approach in order to provide a direct measurement of the energy dissipated by damping in the time domain, with minimum contamination from the interaction effects between specimen and test fixture. It can be readily applied with standard laboratory instrumentation and readily adaptable to realistic simulations of disturbance propagation phenomena through actual structures.

Acknowledgment

This effort was supported by the Air Force Office of Scientific Research on Contract F49620-83-C-0017. The assistance of Mr. Phil Smith in conducting the experiments is gratefully acknowledged.

References

[1]*Second Forum on Space Structures*, sponsored by the Air Force Office of Scientific Research, Air Force Flight Dynamics Laboratory, NASA Langley Research Center, McLean, VA, June 11-13, 1984.

[2]Trudell, R. W., Curley, R. C., and Rogers, L. C., "Passive Damping in Large Precision Space Structures," AIAA/ASME/ASCE/AHS 21st Structures, Structural Dynamics and Materials Conference, Paper 80-0677, Seattle, WA, May 1980, pp. 124-136.

[3]Nakra, B. C., "Vibration Control with Viscoelastic Materials," *Shock and Vibration Digest*, Vol. 8, No. 6, June 1975, pp. 3-12.

[4]Trapp, W. J. and Bowie, G. E., "Perspectives on Damping," *Damping Applications for Vibration Control,* edited by P. J. Torvik, ASME Winter Annual Meeting, Chicago, 1980.

[5]Beards, C. F., "Damping in Structural Joints," *Shock and Vibration Digest,* Vol. 11, No. 9, Sept. 1979, pp. 35-41.

[6]Trudell, R. W., Rehfield, L. W., Reddy, A., Prucz, J., and Peebles, J., "Passively Damped Joints for Advanced Space Structures," Proceedings, Vibration Damping Workshop, Air Force Flight Dynamics Laboratory, Long Beach, CA, Feb. 27-29, 1984.

[7]Trudell, R. W. and Blevins, C. E., "Passively Damped Joints for Advanced Space Structures," Annual Technical Report MDC H1178, McDonnell Douglas Astronautics Company, Huntington Beach, CA, June 1984.

[8]Prucz, J., "Analysis of Design Tradeoffs for Passively Damped Structural Joints," *Journal of Spacecraft and Rockets,* Vol. 23, Nov.-Dec. 1986, pp. 576-584.

[9]Lazan, B. J., *Damping of Materials and Members in Structural Mechanics,* Pergamon Press, Inc., London, 1968.

[10]Read, B. E. and Dean, G. D., *The Determination of Dynamic Properties of Polymers and Composite,* John Wiley and Sons, New York, 1978.

[11]Bert, C. W. and Clary, R. R., "Evaluation of Experimental Methods for Determining Dynamic Stiffness and Damping of Composite Materials," *Composite Materials: Testing and Design* (3rd Conference), ASTM STP 546, 1974, pp. 250-265.

[12]Chu, F. H. and Wang, B. P., "Experimental Determination of Damping in Materials and Structures, *Damping Applications for Vibration Control,* edited by P.J. Torvik, ASME Winter Annual Meeting, Chicago, 1980.

[13]Prucz, J., "Analytical and Experimental Methodology for Evaluating Passively Damped Structural Joints," Ph.D. Dissertation, Georgia Institute of Technology, May 1985.

[14]Clough, R. W. and Penzien, J., *Dynamics of Structures,* McGraw-Hill, Inc., 1975.

[15]Plunkett, R., "Measurement of Damping," *Structural Damping,* Section 5, Ruzicka, J. E., ed., ASME Annual Meeting, Atlantic City, NJ, 1959.

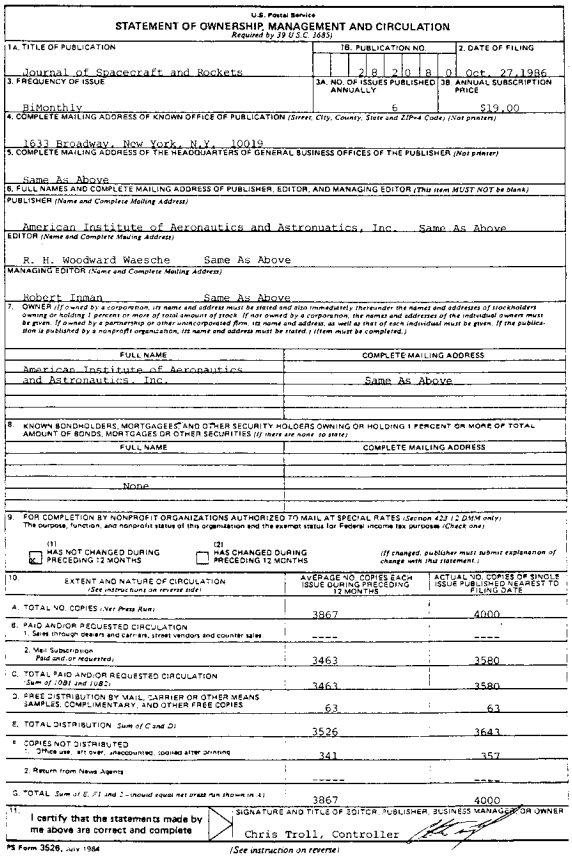

U.S. Postal Service
STATEMENT OF OWNERSHIP, MANAGEMENT AND CIRCULATION
Required by 39 U.S.C. 3685)

1A. TITLE OF PUBLICATION	1B. PUBLICATION NO.	2. DATE OF FILING
Journal of Spacecraft and Rockets	0 0 2 1 8 2 1 0 1 8 0	Oct. 27,1986
3. FREQUENCY OF ISSUE	3A. NO. OF ISSUES PUBLISHED ANNUALLY	3B. ANNUAL SUBSCRIPTION PRICE
BiMonthly	6	$19.00

4. COMPLETE MAILING ADDRESS OF KNOWN OFFICE OF PUBLICATION (Street, City, County, State and ZIP+4 Code) (Not printers)
1633 Broadway, New York, N.Y. 10019

5. COMPLETE MAILING ADDRESS OF THE HEADQUARTERS OF GENERAL BUSINESS OFFICES OF THE PUBLISHER (Not printer)
Same As Above

6. FULL NAMES AND COMPLETE MAILING ADDRESS OF PUBLISHER, EDITOR, AND MANAGING EDITOR (This item MUST NOT be blank)

PUBLISHER (Name and Complete Mailing Address)
American Institute of Aeronautics and Astronautics, Inc. Same As Above

EDITOR (Name and Complete Mailing Address)
R. H. Woodward Waesche Same As Above

MANAGING EDITOR (Name and Complete Mailing Address)
Robert Inman Same As Above

7. OWNER (If owned by a corporation, its name and address must be stated and also immediately thereunder the names and addresses of stockholders owning or holding 1 percent or more of total amount of stock. If not owned by a corporation, the names and addresses of the individual owners must be given. If owned by a partnership or other unincorporated firm, its name and address, as well as that of each individual must be given. If the publication is published by a nonprofit organization, its name and address must be stated.) (Item must be completed.)

FULL NAME	COMPLETE MAILING ADDRESS
American Institute of Aeronautics and Astronautics, Inc.	Same As Above

8. KNOWN BONDHOLDERS, MORTGAGEES, AND OTHER SECURITY HOLDERS OWNING OR HOLDING 1 PERCENT OR MORE OF TOTAL AMOUNT OF BONDS, MORTGAGES OR OTHER SECURITIES (If there are none, so state)

FULL NAME	COMPLETE MAILING ADDRESS
None	

9. FOR COMPLETION BY NONPROFIT ORGANIZATIONS AUTHORIZED TO MAIL AT SPECIAL RATES (Section 422.12 DMM only)
The purpose, function, and nonprofit status of this organization and the exempt status for Federal income tax purposes (Check one)

(1) ☐ HAS NOT CHANGED DURING PRECEDING 12 MONTHS (2) ☐ HAS CHANGED DURING PRECEDING 12 MONTHS (If changed, publisher must submit explanation of change with this statement.)

10. EXTENT AND NATURE OF CIRCULATION (See instructions on reverse side)	AVERAGE NO. COPIES EACH ISSUE DURING PRECEDING 12 MONTHS	ACTUAL NO. COPIES OF SINGLE ISSUE PUBLISHED NEAREST TO FILING DATE
A. TOTAL NO. COPIES (Net Press Run)	3867	4000
B. PAID AND/OR REQUESTED CIRCULATION 1. Sales through dealers and carriers, street vendors and counter sales	----	----
2. Mail Subscription Paid and/or requested	3463	3580
C. TOTAL PAID AND/OR REQUESTED CIRCULATION (Sum of 10B1 and 10B2)	3463	3580
D. FREE DISTRIBUTION BY MAIL, CARRIER OR OTHER MEANS SAMPLES, COMPLIMENTARY, AND OTHER FREE COPIES	63	63
E. TOTAL DISTRIBUTION (Sum of C and D)	3526	3643
F. COPIES NOT DISTRIBUTED 1. Office use, left over, unaccounted, spoiled after printing	341	357
2. Return from News Agents	----	----
G. TOTAL (Sum of E, F1 and 2 - should equal net press run shown in A)	3867	4000

11. I certify that the statements made by me above are correct and complete. SIGNATURE AND TITLE OF EDITOR, PUBLISHER, BUSINESS MANAGER, OR OWNER
Chris Troll, Controller

PS Form 3526, July 1984 (See instruction on reverse)